ChemElectroChem

Review
doi.org/10.1002/celc.202400660

Chemistry Europe
European Chemical Societies Publishing

www.chemelectrochem.org

Graphene Derivatives as Efficient Transducing Materials for Covalent Immobilization of Biocomponents in Electrochemical Biosensors

Petr Jakubec, David Panáček, Martin-Alex Nalepa, Marianna Rossetti, Ruslan Álvarez-Diduk, Arben Merkoçi, Majlinda Vasjari, Lueda Kulla, and Michal Otyepka*

This review highlights the role of graphene derivatives in advancing electrochemical biosensors for applications in diagnostics, environmental monitoring, and industrial sensing. Graphene derivatives, including graphene oxide (GO), reduced GO, and wide range of graphenes prepared via fluorographene chemistry, represent a prominent class of transducing materials in electrochemical biosensor development. Their ability to support covalent immobilization of biocomponents ensures stability, specificity, and long-term performance, addressing limitations of noncovalent methods. Advances in fabrication, such as laser-assisted reduction, enable scalable and cost-effective production of conductive graphene-based electrodes. Covalent functionalization techniques, like carbodiimide coupling and click chemistry, facilitate integration with bioreceptors, leading to highly selective biosensors. Emerging approaches, including inkjet printing of graphene-based inks onto eco-friendly substrates, promise sustainable and portable diagnostic devices. These advances support biosensors aligned with modern and sustainable technologies. Future efforts must focus on scalable production, improved multiplexing, and environmental sustainability to fully harness the potential of graphene derivatives in electrochemical biosensors.

1. Introduction

Electrochemical devices hold significant promise across a wide range of application fields, including healthcare, food production, biosafety, and the monitoring of environmental and industrial processes. Electrochemical sensors, and particularly biosensors, are well suited for these tasks, as they align with the REASSURED principles defined by the World Health Organization for point-of-care (PoC) devices. The REASSURED principles for PoC devices include being Real-time, Easy to use, Affordable, Sensitive, Specific, User-friendly, Rapid, Equipment-free, and Deliverable to end users.[1] Additionally, these devices offer a quantitative response and are easily miniaturized. The success of these technologies is well demonstrated by the widespread use of electrochemical sensors, such as in pH measurement and healthcare applications. A prime example is the glucometer, often considered the archetype of biochemical sensors, as first described by Leland Clark in 1962.[2] According to the The international union of pure and applied chemistry (IUPAC) definition,[3] a biosensor can be described as a self-contained, integrated analytical device. It incorporates a biological recognition element including enzymes, antibodies, peptides, DNA, aptamers, etc. placed in direct spatial contact with a transduction element such as optical or electrochemical transducers (**Figure 1**a,b). One of the key challenges in the future

P. Jakubec, D. Panáček, M.-A. Nalepa, M. Otyepka
Regional Centre of Advanced Technologies and Materials
Czech Advanced Technology and Research Institute (CATRIN)
Palacký University Olomouc
Šlechtitelů 241/27, 783 71 Olomouc, Czech Republic
E-mail: michal.otyepka@upol.cz

D. Panáček
Nanotechnology Centre
Centre of Energy and Environmental Technologies
VŠB–Technical University of Ostrava
17. listopadu 2172/15, 708 00 Ostrava-Poruba, Czech Republic

M.-A. Nalepa
Department of Physical and Macromolecular Chemistry
Faculty of Science
Charles University
Hlavova 2030/8, 128 43 Prague, Czech Republic

M. Rossetti, R. Álvarez-Diduk, A. Merkoçi
Catalan Institute of Nanoscience and Nanotechnology (ICN2)
CSIC and the Barcelona Institute of Science and Technology (BIST)
Campus UAB, Bellaterra, 08193 Barcelona, Spain

A. Merkoçi
ICREA Institució Catalana de Recerca i Estudis Avançats
Pg. Lluís Companys 23, 08010 Barcelona, Spain

M. Vasjari, L. Kulla
Department of Chemistry
Faculty of Natural Sciences
University of Tirana
Tiranë 1000, Albania

M. Vasjari, L. Kulla
NANOBALKAN - NANOALB
Academy of Science of Albania
Tiranë 1000, Albania

M. Otyepka
IT4Innovations
VŠB-Technical University of Ostrava
17. listopadu 2172/15, 708 00 Ostrava-Poruba, Czech Republic

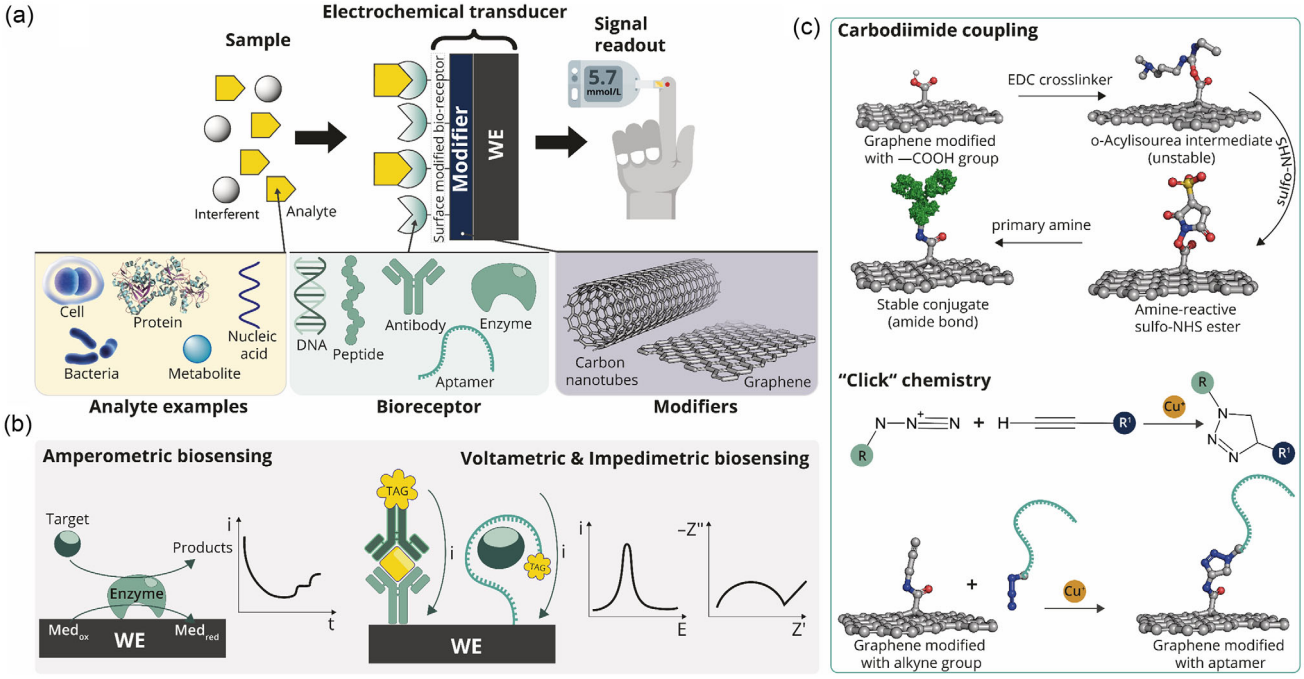

Figure 1. a) Schematic representation of an electrochemical biosensor, comprising a biocomponent integrated with a transducer, whose signal is processed by a readout system. The biocomponent imparts selectivity to the biosensor, while the transducer plays a key role in ensuring sensitivity. b) Representative examples of electrochemical techniques commonly used for biosensor evaluation. Reproduced and adapted under terms of the CC-BY license.[15] Copyright 2022, Elsevier. c) Scheme of bioconjugation strategies including both carbodiimide coupling and "click" chemistry. Reproduced and adapted under terms of the CC-BY license.[16] Copyright 2020, MDPI.

development of biosensors lies in achieving an efficient interface between the biocomponent and the transducer. The interaction between the biocomponent and the transducer is critical for the sensitivity, specificity, and overall performance of a biosensor.[4–6] Efficient binding ensures that a biorecognition element maintains its activity and is appropriately oriented to interact with the target analyte.[7] Moreover, the stable attachment prevents the leaching of the biocomponent, which can lead to signal loss and decreased sensor reliability.[8] The interface between the biorecognition element and transducer can be established via noncovalent or covalent methods. Noncovalent functionalization (i.e., adsorption) is easier to implement but carries the risk of biocomponent disintegration or leakage, which could impair the sensor's performance. In contrast, covalent functionalization offers improved stability but is more challenging to establish. This approach requires specific functional groups on both the biocomponent and the transducer that can be conjugated under mild conditions to avoid damaging the biocomponent, such as through thermal denaturation. The covalent functionalization relies on chemical coupling methods such as carbodiimide coupling[9] and click chemistry.[10] The carbodiimide coupling, using 1-ethyl-3-(3-dimethylaminopropyl) carbodiimide (EDC) and N-hydroxysuccinimide (NHS), facilitates amide bond formation between carboxyl (—COOH) groups on graphene derivatives and primary amines ($—NH_2$) of bioreceptors, making it particularly effective in aqueous environments.[11] The click chemistry, in contrast, enables highly efficient and specific bioconjugation under ambient conditions, preserving the activity of sensitive bioreceptors, with copper-catalyzed azide-alkyne cycloaddition (CuAAC) serving as a prominent example[12,13] (Figure 1c). The choice between these methods depends on factors such as specificity, reaction conditions, and the functional groups available for conjugation. Additionally, chain length of the cross-linker plays a crucial role in determining the orientation, accessibility, and binding efficiency of bioreceptors. Short-chain cross-linkers (e.g., EDC/NHS) provide rigid, close attachment, enhancing electron transfer but potentially interfering with the analyte-binding site of biomolecules, while long-chain cross-linkers (e.g., polyethylene glycol variants (PEGylated)) increase receptor mobility and reduce nonspecific adsorption at the cost of electron transfer efficiency. The optimal cross-linker choice depends on the application, analyte size, and biosensor configuration, with short chains preferred for rapid electron transfer in small biomolecules and longer chains better suited for large proteins or complex biological systems.[14]

Michal Otyepka is a Ph.D. holder and the Head of the Nanomaterial Research Division at CATRIN, Palacký University Olomouc, and leads the Laboratory for Modeling of Nanotechnologies at IT4Innovations, VSB-Technical University, Ostrava. His research focuses on the properties and reactivity of graphene derivatives, 2D materials and carbon dots, as well as their applications in sensing and biosensing, catalysis, and energy storage. He developed the chemistry of fluorographene toward graphene derivatives. He contributed to development of multiscale computational methods to explore nanomaterials and complex molecular systems.

2. Selection of Electrochemical Technique

Selecting the right electrochemical technique for signal acquisition is essential for optimizing the performance of biosensors, especially to ensure high selectivity and sensitivity. The choice of method largely depends on the specific analyte, required detection limits, and the overall design of the sensor. Each electrochemical technique comes with its own set of benefits and limitations, making the selection process delicate for achieving optimal results. Cyclic voltammetry (CV) is widely used for studying redox properties and reaction kinetics, offering insights into electrode modifications and reaction mechanisms.[17,18] Despite its broad utility, CV's high background current and moderate sensitivity limit its applicability for low-concentration analytes. Nonetheless, CV remains essential in enzymatic biosensors for verifying the immobilization of catalytic biomolecules.[19–21] Differential pulse voltammetry (DPV) improves sensitivity minimizing background noise and enhancing peak resolution. DPV is particularly useful for distinguishing structurally similar compounds, such as neurotransmitters, in complex biological samples.[22,23] However, electrode fouling can reduce performance, necessitating surface modifications for long-term stability.[24] Square-wave voltammetry (SWV) enhances sensitivity by maximizing signal-to-noise ratios, making it ideal for rapid analysis and environmental monitoring.[25,26] In heavy metal detection, SWV differentiates well multiple metal ions, such as Pb^{2+} and Cd^{2+}, by generating distinct electrochemical signatures.[27] Beyond voltammetric techniques, electrochemical impedance spectroscopy (EIS) enables real-time, label-free monitoring of molecular interactions.[28,29] Unlike direct electron transfer-based techniques, EIS detects impedance changes induced by biomolecular binding, making it ideal for DNA hybridization assays and pathogen detection.[30,31] While EIS provides high selectivity, its application is limited by complex data interpretation, requiring advanced signal processing techniques.[32–34]

2.1. Carbon-Based Transducers

Carbon-based materials are highly competitive as transducers for biosensing, offering required properties while being composed of earth-abundant element, which contributes to their low environmental impact.[35] Among them, 2D graphene stands out due to its large surface area and excellent electronic properties.[36] Graphene can be synthesized using various methods, broadly classified into top-down and bottom-up approaches.[37] The bottom-up approach includes chemical vapor deposition, where graphene is grown on metal substrates like copper by decomposing hydrocarbon gases at high temperatures, yielding large size films of monolayer graphene.[38] The top-down approach includes mechanical exfoliation, where layers of graphene are mechanically peeled from graphite, and electrochemical and chemical exfoliation utilizing solvents and external forces (e.g., induced by sonication) delaminating graphite.[39,40] It should be noted that during graphene synthesis impurities, defects and functional groups can be introduced into the ideal graphene honeycomb lattice.[41,42] So each synthesis method influences the structural, electrical, and chemical properties of graphene, making it essential to select the appropriate technique based on the intended biosensor application.[43–46] Graphene is a highly promising transducing material, but its functionalization with biocomponents is typically achieved via noncovalent methods. A prototypical example is the attachment of (SARS-CoV-2) severe acute respiratory syndrome-corana virus-2 spike antibody using pyrenebutyric acid, which interacts with graphene via π–π stacking.[47] However, direct covalent functionalization of graphene is difficult due to its low chemical reactivity.[48,49] Though, it can be realized by strong processes including ion-sputtering generation of radicals,[50–52] cold plasma,[53] and strong oxidizing agents.[54] Various useful graphene derivatives can also be prepared by the direct graphene functionalization using wet chemistry including, e.g., graphene oxide (GO) and fluorographene (FG). A subsequent focus will be directed toward this wet chemical approach, which can be scaled up for the production of cost-effective biosensor electrodes.

2.2. Graphene Oxide

GO is particularly appealing for electrochemical sensing because its oxygen-containing functional groups allow for specific interactions with analytes and provide sites for conjugation with biocomponents.[43] However, GO's nonconductive nature limits its use in electrochemical applications. Conductivity can be restored through chemical or thermal reduction, resulting in (chemically or thermally) reduced GO (rGO). GO is synthesized by oxidizing graphite using strong oxidants, typically via Hummers' method.[55,56] Graphite is treated with sulfuric acid (H_2SO_4) and potassium permanganate ($KMnO_4$), introducing oxygen functional groups that make it hydrophilic. The reaction is quenched with water and hydrogen peroxide (H_2O_2), followed by purification.[57] GO sheets are then exfoliated into single layers via ultrasonication or mechanical stirring. The synthetic methods used for manufacturing of GO inevitable introduce various oxygen containing functions (e.g., epoxy, hydroxy, carboxy) on graphene. Still, the complex chemical composition of GO and its derivatives, with various functional groups, poses another challenge for utilization of these materials in electrochemical applications. GO and its various reduced forms have been successfully used in various biosensing applications, which are overviewed in wealth in literature.[43,44] To improve and simplify rGO electrodes production, Merkoci's group developed a print-stamp laser-assisted technology that enables in situ laser-induced reduction and patterning of GO to create highly conductive rGO films,[58] offering a groundbreaking alternative to the traditional methods. By using a CO_2 laser, this method allows to directly reduce and pattern GO films in a solvent-free single step, producing highly exfoliated and conductive rGO structures without the need for extensive thermal or chemical processes. This technology is scalable, cost-effective, and environmentally friendly, making it an innovative solution for biosensor development and other graphene-based applications. Furthermore, by utilizing metal salts as precursors, the process simultaneously reduces GO and generates composites with metal nanoparticles (MNPs), such as gold, silver, or platinum (**Figure 2**a). The resulting hybrid nanocomposites, with MNPs

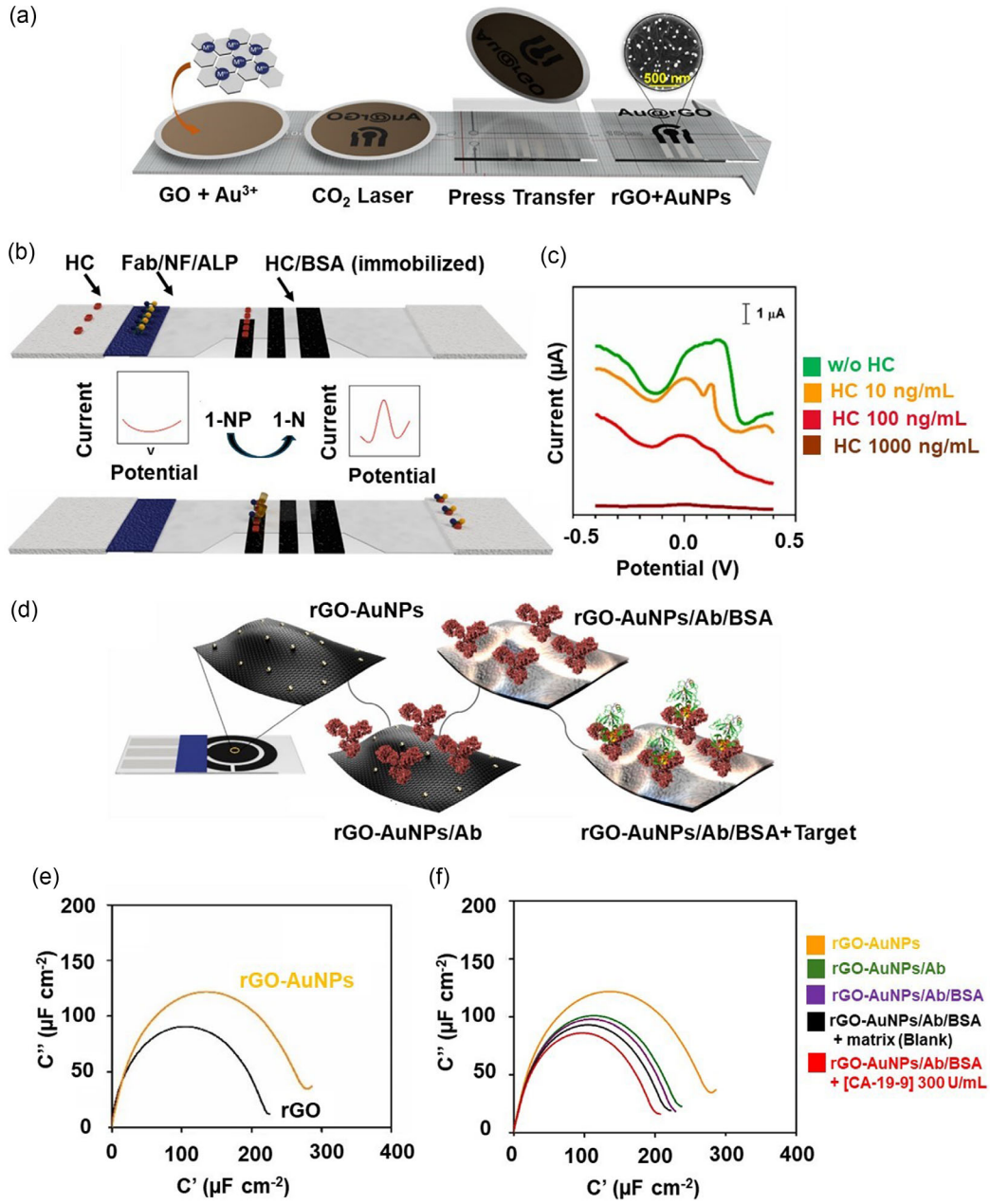

Figure 2. a) Schematic illustration of the fabrication process of nanostructured rGO–AuNP electrodes. A GO–Au^{3+} film is prepared by incorporating gold cations (Au^{3+}) into a GO matrix. The film is then patterned and reduced using a CO_2 laser to obtain a conductive rGO film decorated with gold NPs (AuNPs). Finally, the patterned rGO-AuNP film is transferred onto a polyethylene terephthalate (PET) substrate, where silver ink electrical connections are screen-printed. The inset shows a high-resolution microscopic image of AuNPs distributed on the rGO surface. b) Schematic illustration of the electrochemical sensing mechanism based on enzymatic amplification approach using alkaline phosphatase (ALP). The sensing platform is functionalized with antibodies (Fab) conjugated with Au–IrO_2 nanoflowers (NF) and alkaline phosphatase (ALP) for target detection. A change in the electrochemical signal is observed upon target binding. Specifically, hydrocortisone (HC) in the sample competes with immobilized HC/BSA for binding to anti-cortisol Fab conjugated with NFs and ALP at the test line (TL). After washing, 1-naphthyl phosphate (1-NP), a non-electroactive substrate, is introduced near the TL and the working electrode. The enzymatic reaction converts 1-NP into electroactive 1-naphthol (1-N), which is detected by DPV, generating a measurable signal. c) Raw DPV profiles of the sensor at different concentrations of the target biomarker (HC), demonstrating a concentration-dependent signal increase. d) Schematic illustration of the functionalization steps of rGO–AuNP electrodes with CA-19-9 antibodies for the electrochemical detection of a pancreatic cancer biomarker using quantum capacitance spectroscopy: initial rGO–AuNPs, immobilization of antibodies (Ab), blocking with bovine serum albumin (BSA), and target biomarker recognition. e) Capacitive Nyquist plots comparing the capacitance of rGO and rGO–AuNP electrodes in 50 mM phosphate-buffered saline (PBS)/0.1 M KCl pH 6.0, 10 mV amplitude sinusoidal perturbation, and frequency range from 100 kHz to 0.1 Hz, highlighting the enhanced electrochemical properties of the nanostructured surface. f) Capacitive Nyquist plot showing the effect of sequential functionalization steps on the capacitance, confirming successful biomolecule immobilization and target recognition. Adapted with permission.[58,60,61] Copyright 2020 and 2024, IOP Publishing and Elsevier.

embedded within rGO, can be seamlessly transferred onto various substrates and possess excellent properties such as improved conductivity and catalytic activity, making them well suited for biosensing applications.[59] The laser-fabricated rGO electrodes can be directly integrated into nitrocellulose strips of lateral flow assays (LFAs)[60] (Figure 2b) for sensing applications. By utilizing a

roll-to-roll transfer mechanism, the deposition of rGO onto nitrocellulose is seamless securing fluidic properties necessary for LFAs. The laser-based approach also allows creating trapezoidal windows to expose the nitrocellulose backing, facilitating leak-proof connections to potentiostat. Such innovations address scalability challenges and enhance the precision of electrochemical measurements, expanding the potential of graphene related materials for low-cost, accessible diagnostic solutions, as demonstrated by the electrochemical analyte detection via enzymatic reactions (Figure 2c). rGO can integrate with various materials, including metal and semiconductor nanoparticles, metal oxides, organic molecules, dopants, quantum dots, and polymers, to form nanocomposites with superior electrical properties and functional versatility. This versatility is widely harnessed for functionalizing rGO with bioreceptors, facilitating the development of electrochemical biosensors, such as enzymatic sensors, DNA-based biosensors, and immunosensors. Despite these advancements, the covalent modification remains limited, with most rGO-based biosensors still relying primarily on adsorption for bioreceptor immobilization. Recently, the first capacitive immunosensor that utilizes rGO-AuNP electrodes fabricated by laser-scribing covalently functionalized with carbohydrate antigen (CA)-19-9 antibodies (through thiol-gold chemistry) was successfully used for detection of CA-19-9 glycoprotein, a key pancreatic cancer biomarker (Figure 2d).[61] The detection relied on quantum capacitance transduction, in which molecular recognition events modify the electrode's density of states, leading to detectable changes in capacitance.[62] Indeed, the nanostructured rGO films exhibit notable quantum capacitance (214 $\mu F\ cm^{-2}$), attributable to the density of electronic states within the conjugated π-orbital system. Incorporating gold nanoparticles (AuNPs) into the rGO matrix further increases this value to 265 $\mu F\ cm^{-2}$ by creating efficient pathways for electron transfer between graphene layers and the current collector (Figure 2e). This increase in quantum capacitance is crucial for detecting molecular interactions at the electrode surface, making rGO–AuNP electrodes highly effective for electrochemical biosensing.[63] Based on the differential capacitance response, which depends on target concentration, the proposed immunosensor show a linear dynamic range of 0–300 $U\ mL^{-1}$ and a limit of detection as low as 8.9 $U\ mL^{-1}$ (Figure 2f). A significant advancement in electrochemical biosensing has been also demonstrated with the development of a label-free and amplified electrochemical impedimetric aptasensor utilizing functionalized graphene nanocomposites (rGO–AuNPs) for thrombin detection. This sensor exhibited a linear response to thrombin concentrations ranging from 0.3 to 50 nM, achieving an impressive detection limit of 0.01 nM.[64] The potential of rGO in biosensing applications is further illustrated by the work of Dinani et al.[65] who developed an aptasensor based on an AuNPs/Fe_3O_4/rGO nanocomposite for the detection of miRNA 128, a biomarker associated with acute lymphoblastic leukemia. This system demonstrated an extraordinary detection range from 0.01 to 0.09 fM, reaching a detection limit as low as 0.005483 fM. Beyond these specific applications, the versatility of rGO-based biosensors has been extensively documented in numerous reviews, covering a broad spectrum of practical implementations, including bacterial detection,[66] medical diagnostics,[67] and environmental monitoring.[68]

2.3. Fluorographene Chemistry

FG is another valuable graphene derivative, produced by the direct fluorination of graphene or by the chemical or mechanical exfoliation of graphite fluoride, which is commonly used as a dry lubricant or as an electrode material in primary lithium batteries.[69] Being perfluorinated hydrocarbon, with stoichiometry of $C_1F_{1.1}$, it was regarded as the counterpart of perfluoroethylene (marketed also as Teflon).[70] FG is composed of fluorine atoms attached to tertiary carbon atoms in sp^3 hybridization.[71] This material is nonconductive, being considered one of the thinnest insulators with an electronic bandgap of 8.5 eV[72] and optical bandgap of 5.75 eV.[73] It also naturally contains various defects, which make FG electron acceptor susceptible for wide range of reactions.[74,75]

The reactions of FG include two major reaction channels, i.e., reductive defluorination and substitution.[75] These reactions, which usually occur simultaneously, yield graphene derivatives with varying degrees of functionalization, from a few to 20%–30%, depending on the conditions. The resulting materials feature a combination of sp^2/sp^3 carbons and covalently attached functional groups. The nature of the functional group depends on the reactants used during FG treatment.

FG functionalization typically occurs via wet chemistry approaches, with solvents playing a significant role in determining the degree of functionalization. For instance, solvents like ortho-dichlorobenzene and alkanes result in low degrees of functionalization, whereas dimethylformamide (DMF) enables a higher level of functionalization, producing nearly fluorine-free materials.[74] However, DMF is under scrutiny due to EU (REACH) registration, evaluation, authorization, and restriction of chemicals regulation aimed at protecting human health and the environment from chemical risks, which places stricter requirements on chemicals of concern. Consequently, eco-friendly alternatives like N-butylpyrrolidone are preferred for industrial applications. The FG functionalization typically occurs at mild temperatures below 130 °C, providing controllable reaction conditions that can be easily standardized, with scalability demonstrated in batches of up to 1 kg.

The controlled chemistry and scalability of FG make it highly attractive for sensing[76,77] and biosensing applications,[78] because it can produce graphene lattice with surface-grafted functional groups. Numerous functional groups have already been successfully grafted onto graphene surfaces, and their properties have been thoroughly reviewed in specialized literature.[69,79,80] Dual[81,82] and Janus (one-sided)[83] modes of functionalization have also been reported, expanding the range of possible applications. FG chemistry is further extended to produce also in-lattice-doped graphene derivatives, such as nitrogen-doped graphenes.[84,85] Chemical processes leading to both in-plane doped and functionalized graphene derivatives have also been developed, and nitrogen-doped graphene acid (NGA)[77] represents a prototypical member of this family.

Functionalization of FG effectively circumvents the low intrinsic reactivity of graphene, leading to the synthesis of graphene derivatives with homogeneously surface-grafted organic functional groups. Notably, carboxyl and ethynyl groups are

significant because they can be efficiently utilized for subsequent conjugation with biocomponents via carbodiimide-mediated coupling[78] or click chemistries such as CuAAC.[86] The mild conjugation with biocomponents opens door for efficient and versatile biosensing applications with discussed graphene derivatives.

2.4. Graphene Acid

Graphene acid (GA), i.e., graphene derivative densely functionalized with carboxyl groups (with a degree of functionalization of ≈10%), has demonstrated exceptional suitability for biofunctionalization. GA is equipped with a conductive structure with a sheet resistance of 6800 Ω sq^{-1} measured by a four-probe technique on a 7 μm thick film, which was five orders of magnitude higher than the sheet resistance of GO.[87] EIS displays 40 times lower resistivity of GA with $R_{ct} = 81\ \Omega$ when compared with GO ($R_{ct} = 3542\ \Omega$). CV with 5 mmol L^{-1} $[Fe(CN)_6]^{3-/4-}$ redox probe also documented conductivity of GA and also indicated on capacitive behavior, which can be utilized in supercapacitors[88–90] (**Figure 3**).

GA, with its electrochemical properties and presence of carboxyl groups, which can be utilized for bioconjugation via carbodiimide chemistry, provides an optimal platform for immobilizing, e.g., DNA probes. GA was conjugated with single-stranded DNA targeting pork mitochondrial DNA, forming a stable amide bond via the carbodiimide coupling (**Figure 4**). This robust functionalization allowed the creation of a label-free, reagentless electrochemical genosensor that utilized non-Faradaic impedance spectroscopy for rapid detection. The platform achieved a detection limit of 9% w/w pork content in beef samples without requiring DNA amplification or purification and retained its functionality for at least 4 weeks. This methodology demonstrates the potential for developing scalable, eco-friendly biosensing platforms applicable to various fields, e.g., food safety and medical diagnostics.[78]

GA can also be modified for conjugation via click chemistry, which significantly enhances its versatility as a transducing material in the construction of biosensors. To achieve this, an alkyne group was first introduced to GA via its conjugation with propargylamine via carbodiimide chemistry.[86] This material (GA–NH–YN) allowed subsequent conjugation with a modified aptamer selective for ampicillin binding (**Figure 5**). The resulting material was utilized for electrode modification, enabling the development of a highly selective and sensitive platform for ampicillin detection (Figure 5). SWV was conducted at a high frequency of 100 Hz and a low amplitude of 10 mV. This configuration produced a "signal-on" response, characterized by an increase in the recorded current upon binding of ampicillin (in its zwitterionic form) to the aptamer. The binding induced a conformational change that reduced the distance between the redox probe attached to the aptamer and the electrode surface and increased an electron transfer rate. This setup achieved a detection limit of 1.36 nM, which is eight times lower than the European Union's maximum residue limit for ampicillin in milk. The material demonstrated excellent capability for nanomolar detection of ampicillin in complex matrices. The biosensing platform enabled direct analysis of biological samples, such as 50% diluted saliva and milk, without requiring extensive pretreatment. Moreover, the developed material and method highlighted the potential for miniaturization and integration into portable sensing devices, paving the way for PoC diagnostics and in-field monitoring applications. The system's robustness, high sensitivity, and compatibility with click chemistry offer a versatile framework for designing future biosensors capable of targeting a wide range of analytes in similarly challenging sample environments.

2.5. Mechanism of Analyte Binding

Gaining detailed structural insights into analyte binding to an aptamer, which could guide aptamer design, remains a significant challenge for research. Experimental techniques, such as nuclear magnetic resonance (NMR) and circular dichroism, provide valuable information in this regard. Complementing these, computational modelling techniques offer unique perspectives on the structural details of such binding. However, despite advancements in predicting biomolecular structures exemplified by AlphaFold[91] current tools still fall short of providing robust

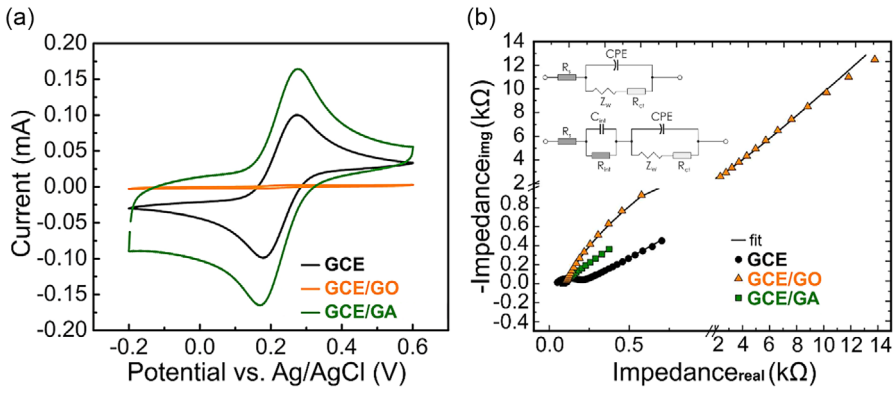

Figure 3. a) CV curves of a bare GCE electrode (black line) and GCE electrodes modified with GO (orange line) or with GA (green line). The CV curve of GA is symmetric and scan-rate independent, indicating reversible behavior with no parallel chemical reactions. b) Electrochemical impedance spectroscopy (EIS) measurements demonstrate the conductive nature of GA. Inset: Nyquist plots for a bare glassy carbon electrode (GCE) and electrodes modified with GO or GA, and Randles equivalent circuit for data fitting. Adapted with permission.[87] Copyright 2017, The American Chemical Society.

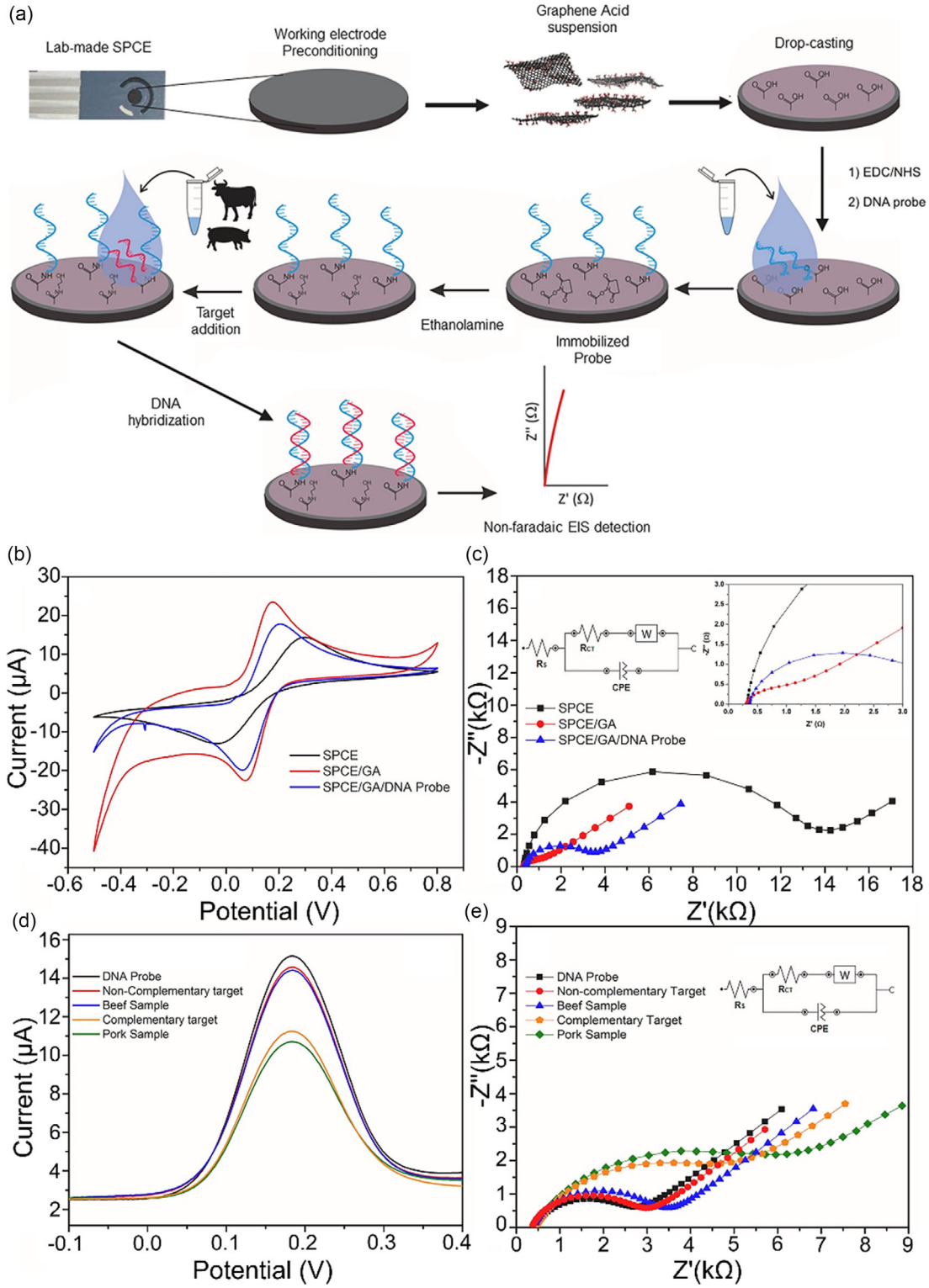

Figure 4. a) Scheme of construction of label-free, reagentless electrochemical genosensor for meat adulteration detection. A screen-printed carbon electrode (SPCE) was modified by drop-casting with GA suspension. The pork DNA recognition biomolecule was attached to the surface by carbodiimide chemistry and ethanolamine was used as blocking agent. Complementary and noncomplementary DNA, as well mixtures of beef and pork samples were added to the surface, incubated, and washed. The detection was performed by non-Faradaic EIS. Electrochemical characterization of the genosensor construction steps: b) cyclic voltammograms of the bare SPCE, SPCE modified with GA (SPCE/GA), and SPCE/GA after the immobilization of the DNA probe (SPCE/GA/DNA Probe). c) Nyquist plots obtained by EIS analysis in each genosensor construction step; inset 1: equivalent Randles circuit, where R_S, R_{CT}, W, and CPE represent the solution resistance, the charge-transfer resistance, the Warburg diffusion resistance, and the constant phase element, respectively; inset 2: high-frequency region zoom. Faradaic detections of complementary target and meat samples: d) square-wave voltammograms and e) Nyquist plots obtained by EIS; inset: equivalent Randles circuit. Electrolyte: PBS (10 mmol L^{-1}), containing $K_4[Fe(CN)_6]$ and $K_3[Fe(CN)_6]$ (1 mmol L^{-1}). CV parameters: potential range from −0.5 to 0.8 V, scan rate 50 mV s^{-1}. EIS parameters: frequency range from 10,000 to 0.1 Hz, potential applied 0.12 V, amplitude 10 mV. SWV parameters: potential range from −0.1 to +0.4 V, amplitude of 25 mV, increment of 4 mV, and frequency of 15 Hz. Adapted with permission.[78] Copyright 2022, Elsevier.

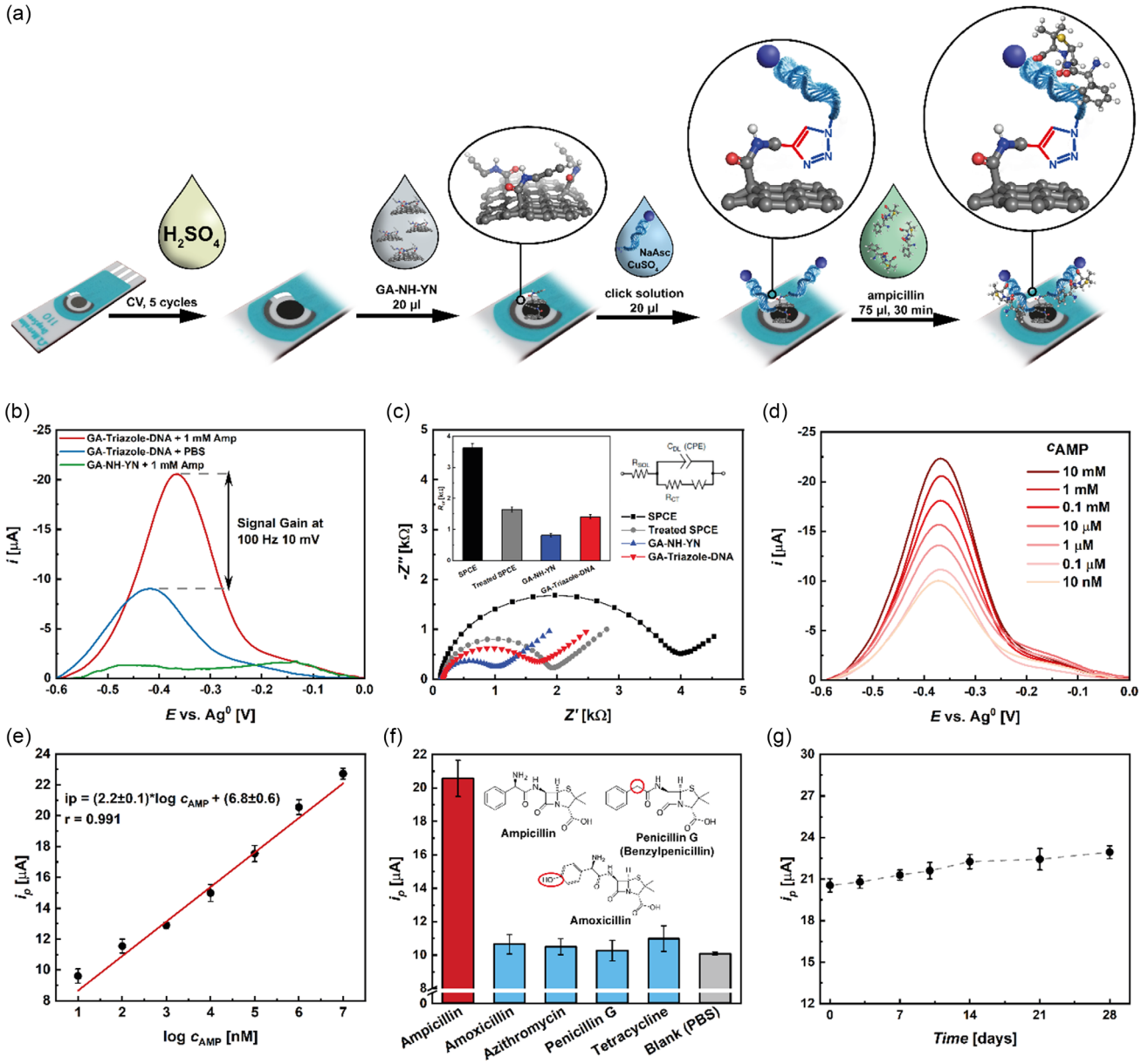

Figure 5. a) Construction scheme of ampicillin aptasensor. SPCE preconditioned with H_2SO_4 was functionalized with GA-NH-YN. Next, click reaction between alkyne groups of this derivative and azide-modified aptamer was performed in the presence of sodium ascorbate (NaAsc) and copper sulfate ($CuSO_4$), resulting in the formation of triazole ring and GA–triazole–DNA conjugate. For the detection, ampicillin solution was left to incubate for 30 min on the electrode. Ampicillin aptasensor performance: b) square-wave voltammograms of methylene blue reduction with optimized parameters (100 Hz, 10 mV) with/without ampicillin and in the absence of aptamer. c) Impedance spectra recorded at various stages of the biosensor construction with redox probe (5 mM $[Fe(CN)_6]^{3-/4-}$ in 10 mM PBS solution, pH = 7.4). d) Representative square-wave voltammograms of the response of the aptasensor in the presence of different ampicillin concentrations. e) Calibration curve of the aptasensor. f) Negative control tests, with the structural analogues of the ampicillin. g) Stability of the response over time study. All potentials are versus metallic silver. Reproduced under terms of the CC-BY license.[86] Copyright 2023, Wiley.

and reliable structural predictions for nucleic acids.[92] Over recent decades, substantial progress has been made in molecular dynamics simulations of nucleic acids[93,94] offering fine special and temporal resolution and hence unique insights into their structure and dynamics.[95] Advanced sampling methods, such as replica exchange molecular dynamics, have the potential to predict conformations[96] and their alterations upon analyte binding. However, even with these advancements, such predictions remain challenging even for short oligonucleotides. For instance, attempts to fully understand the conformational changes following ampicillin binding to the aptamer discussed earlier have provided views into potential interaction sites, but a clear and comprehensive structural picture remains elusive.[86] When nucleic acids interact with the electrode surface, conformational changes can occur due to specific surface interactions (see, e.g., ref. [97]), which make predictions of conformational changes after analyte binding even more challenging. All these facts highlight the need for intensified research efforts in this field, as it holds the potential to significantly advance the rational design of aptamers and hence biosensors.

2.6. Applications in Environment and Industry

Beyond biomedical applications, graphene and its derivatives have demonstrated significant potential in environmental monitoring and industrial sensing. GO and rGO have been extensively used for detecting heavy metal ions (e.g., Pb^{2+}, Cd^{2+}, Hg^{2+}) due to the complexation with surface oxygenous functional groups and high adsorption capacity.[98,99] Heteroatom doping, modification with metal oxides or binding of specific bioreceptors further enhances selectivity of graphene derivatives through chemical affinity and cavity entrapment, enabling precise detection of a wide range of toxic metal ions such as As^{3+}, Cu^{2+}, or Cr^{3+} in complex environmental matrices.[100] Functionalized graphene-based electrodes have also been used for the electrochemical detection of pesticides (e.g., imidacloprid, paraquat, methyl parathion) and persistent organic pollutants (antibiotic residues, hormones, steroid compounds) using both π–π interactions of graphene with aromatic contaminants and covalent immobilization of enzymatic and aptamer-based bioreceptors.[101,102]

In industrial settings, graphene-enhanced gas sensors exhibit remarkable sensitivity for volatile organic compounds (VOCs) and hazardous gases (e.g., NO_x, SO_2). The high surface-to-volume ratio of graphene materials allows for rapid adsorption–desorption kinetics, translating into fast response times and low detection limits.[103] Graphene-based composites incorporating MNPs or metal oxides further enhance electrocatalytic properties, improving industrial sensor performance in detecting process-related contaminants such as hydrogen sulfide (H_2S), ammonia (NH_3), carbon monoxide (CO), and VOCs like methane and toluene, which are critical for workplace safety and emissions monitoring.[104,105] Chemiresistive GO nanocomposites have shown strong potential for detecting hazardous industrial gases like formaldehyde and benzene, enabling real-time monitoring in workplaces.[106]Additionally, the development of flexible graphene-based sensors allows for portable and on-site industrial safety assessments, reducing the risk of prolonged exposure to toxic emissions.[107]

2.7. Wearable Devices

Apart from well-established applications in biomedical, environmental, and industrial sensing, graphene derivatives are also promising candidates in the emerging field of wearable technology, offering a unique combination of flexibility, conductivity, and biocompatibility. While early research demonstrated the feasibility of graphene-based flexible sensors, recent advancements have enabled real-time monitoring of key physiological, chemical, and mechanical parameters.[108] Strain sensors measure muscle movement and joint motion, sweat-based biosensors detect glucose and lactate levels, and gas sensors monitor hazardous gases such as ammonia and acetone.[109,110] GO, rGO, and doped graphene derivatives, such as nitrogen-doped graphene and fluorinated graphene, have been successfully integrated into wearable strain sensors for motion tracking, electrophysiological sensors for electrocardiograph (ECG) and electromyography (EMG) monitoring, and gas sensors for detecting exhaled biomarkers.[110,111] Additionally, hybrid graphene composites with MNPs or conductive polymers are being explored for wearable electrochemical biosensors, particularly for noninvasive glucose monitoring and sweat-based biomarker detection.[111,112] Overall, as the demand for noninvasive monitoring and personalized healthcare continues to grow, graphene derivatives have strong potential to drive this field closer to real-world applications.

2.8. Biocomponent and Transducer Integration

The development of a biosensor requires the integration of a biocomponent with a transducer to form an electrode. In research laboratories, this is often achieved through drop-casting a graphene derivative combined with the biocomponent onto a screen-printed electrode, typically made of carbon or noble metals.[113–115] These electrodes, fabricated on ceramic or plastic substrates, are widely commercially available. However, their widespread use in medical applications poses environmental concerns, primarily due to the persistence of nonbiodegradable support materials. This necessitates the design and fabrication of more sustainable alternatives, which can be achieved by depositing electrode materials onto eco-friendly substrates. Additionally, the use of precise and ideally metal-free electrode materials is crucial for advancing such technologies. Inkjet printing presents a sustainable alternative to conventional electrode fabrication methods, primarily due to its additive manufacturing approach, which minimizes material waste. Unlike subtractive techniques, which generate significant chemical waste due to etching and masking steps, inkjet printing eliminates hazardous byproducts.[116] Compared to screen printing, inkjet printing offers higher material efficiency by depositing material only where needed, minimizing excess ink usage. In contrast, traditional screen printing generates significant toxic chemical waste, not only from excess ink but also from the use of polyester or rubber printing plates and toxic solvents required for roller ink removal.[117,118] In addition, inkjet printing significantly reduces the amount of the main active component needed, requiring only 5–10 wt% compared to 12–20 wt% in screen printing. Unlike screen printing, which relies heavily on binders (45–65 wt%), inkjet printing uses minimal binder and additives, with the ink consisting mostly of solvent (65–95 wt%). This reduction in polymeric binders simplifies ink formulation and helps preserve the functionality of the nanomaterial component, making inkjet printing a more sustainable approach.[119] It offers high accuracy and minimal material waste, requiring only an inkjet printer, suitable ink, and a substrate, without the need for additional equipment or complex processing steps. Since printing is conducted at atmospheric pressure without requiring a vacuum, it significantly reduces energy consumption and operational costs, making it an efficient and cost-effective method for precise fabrication.[120]

2.9. Inkjet Printing Technology

While inkjet printing technology has matured significantly with widely available commercial printers, the choice of appropriate substrate and namely ink formulation remains critical.[121,122]

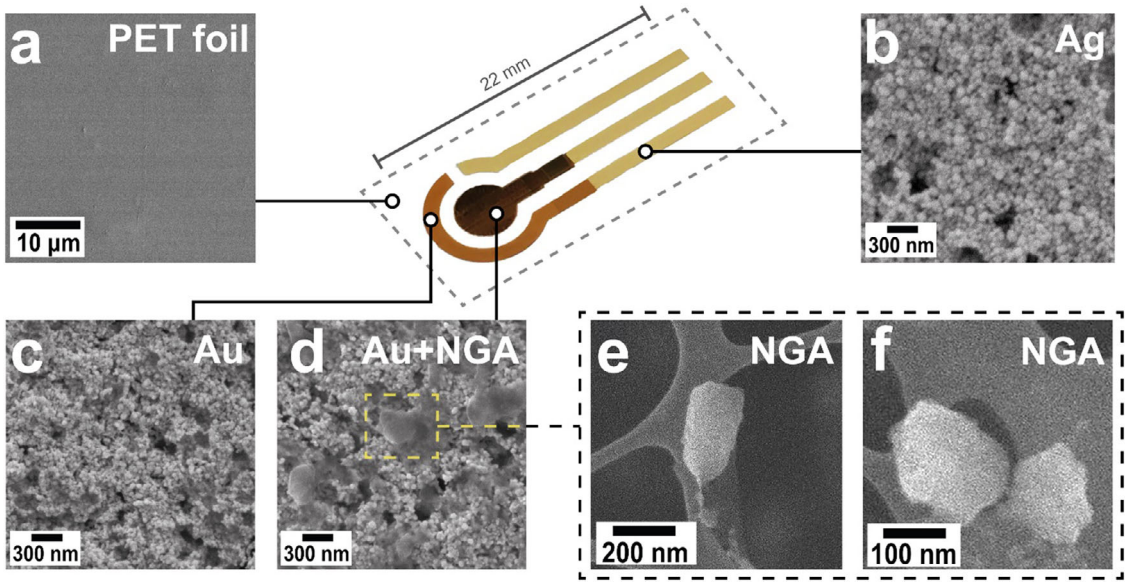

Figure 6. a) SEM characterization of inkjet-printed electrode for dopamine detection. All parts are printed onto PET foil. b,c) Images of silver nanoparticle ink (used for contacts and reference electrode) and gold nanoparticle ink (used for working and counter electrodes) patterns show that silver and gold parts are made up of evenly distributed nanoparticles tens of nanometers in size. d) After inkjet printing of the NGA ink onto already printed Au layer, e,f) the surface of the gold working electrode is also evenly covered with NGA flakes of ≈300 nm in size. Reproduced under terms of the CC-BY license.[127] Copyright 2024, Elsevier.

Regarding substrates, paper stands out as a sustainable, abundant, and low-cost substrate, making it a viable option. Moreover, the potential for printing on biodegradable substrates, such as cellulose-based materials and polylactic acid films, supports the development of fully recyclable and eco-friendly sensor platforms.[123] However, formulating suitable inks poses the greatest challenge. Inks must meet specific physicochemical requirements dictated by the printer's printhead, such as viscosity and surface tension.[124,125] Typically, these inks are colloidal solutions composed of a solvent and dispersed materials. Water-based, additive-free inks further enhance sustainability by eliminating the need for organic solvents such as N-methyl-2-pyrrolidone and DMF, which are commonly used for screen-printable ink formulations.[126] Hence, the dispersed electrode material must form a stable colloidal dispersion in water without causing printhead clogging. Modern printheads can reliably print materials with particle sizes below ≈500 nm. Graphene derivatives are particularly well-suited for this purpose, as they can be reduced to such sizes, functionalized with hydrophilic groups (to form water-stable colloidal dispersions), and exhibit desirable electrochemical properties. These characteristics make graphene derivatives ideal candidates for ink formulations in inkjet-printing-based sensors fabrication.

Recent research demonstrated the feasibility of using NGA as an inkjet-printable material for dopamine detection sensors (**Figure 6**).[127] Several graphene-based inks have already been introduced, although many of these inks have to be optimized by additives.[128–131] However, modern printing inks should be water based and additive free to lower the environmental impact. A step forward has recently been made by Silvestri et al. who used electroactive and self-assembling inkjet-printable ink based on protein–nanomaterial composites and exfoliated graphene for hydrogen peroxide detection.[132] However, the complete fabrication of a fully inkjet-printed biosensor electrode remains unachieved. Further advancements in this area are critical for developing scalable, sustainable, and practical biosensors for real-world applications, unleashing the potential of this method for biosensor design.

3. Summary and Outlook

The future of graphene-based transducers in electrochemical biosensors offers significant opportunities, driven by key advancements in the field. A primary focus lies in enhancing functionalization methods to enable robust covalent immobilization of biocomponents, ensuring high sensitivity and long-term operational stability. Miniaturization and integration into portable platforms are crucial for developing user-friendly devices, particularly for PoC diagnostics and environmental monitoring. The incorporation of multiplexed detection capabilities holds the potential to transform diagnostics by allowing simultaneous identification of multiple analytes, thereby streamlining complex analyses. Addressing the challenges of long-term stability and reusability remains critical to ensure consistent performance over extended periods. On a larger scale, upscaling the synthesis of graphene derivatives is essential to transition from laboratory-scale research to commercially viable technologies, facilitating broader accessibility and application. The development of sustainable electrode materials, replacing traditional metals and environmentally persistent materials with eco-friendly alternatives, aligns with increasing environmental priorities. Innovations such as inkjet-printable graphene-based inks on biodegradable substrates offer promising pathways toward scalable, sustainable,

and cost-effective biosensor fabrication. These advancements collectively improve the performance and practicality of graphene-based biosensors, bringing them closer to commercially viable technologies utilizable in healthcare, environmental monitoring, and industrial applications.

In summary, the overviewed research achievements suggest significant progress toward the development of versatile technologies for constructing graphene-based electrochemical biosensors, although their full realization remains a challenge. Ongoing advancements in graphene-based transducers and their derivatives offer substantial potential for enhancing biosensor performance through innovative functionalization strategies. The combination of scalability, tunable chemistry, and advanced material properties establishes graphene derivatives as a critical component in the future of electrochemical sensing. Furthermore, these materials hold considerable promise for driving technological progress toward sustainable electrochemical biosensing solutions.

Acknowledgements

This work was supported by the ERDF/ESF project TECHSCALE (grant no. CZ.02.01.01/00/22_008/0004587) and ERDF/ESF project "Interdisciplinary Approaches to the Prevention and Diagnosis of Viral Diseases" (grant no. CZ.02.01.01/00/23_021/0008856). The authors also acknowledge financial support from the European Union through the REFRESH project—Research Excellence for Region Sustainability and High-tech Industries (grant no. CZ.10.03.01/00/22_003/0000048), funded via the Operational Programme Just Transition. Additional funding was provided by the European Union's Horizon Europe research and innovation programme (project GRADERINK no. 101137959). This work has received also funding from the European Union's Horizon Europe research and innovation program (SUSNANO) under grant agreement no. 101059266 and from the European Union's Horizon Europe – the Framework Programme for Research and Innovation (2021–2027) under grant agreement No 101120706 (2D-BioPAD). The views and opinions expressed are however those of the author(s) only and do not necessarily reflect those of the European Union. Neither the European Union nor the granting authority can be held responsible for them. The ICN2 is funded by the CERCA programme/Generalitat de Catalunya. The ICN2 is supported by the Severo Ochoa Centres of Excellence programme, Grant CEX2021-001214-S, funded by MCIU/AEI/10.13039.501100011033. We acknowledge Departament de Recerca i Universitats of Generalitat de Catalunya for the grant 2021 SGR 01464. We also acknowledge grant PID2021-124795NB-I00 funded by MICIU/AEI/10.13039/501100011033 and by "ERDF/EU".

Conflict of Interest

MO has share in biosimulation company InSiliBio and supercaps company ATOMIVER.

Author Contributions

Petr Jakubec: visualization (equal); funding acquisition; and writing—original draft (supporting); **David Panáček**: visualization (equal); writing—original draft (supporting); and writing—review and editing (supporting). **Martin-Alex Nalepa**: visualization (equal) and writing—original draft (supporting). **Marianna Rossetti**: visualization (equal); writing—original draft (equal); and writing—review and editing (supporting). **Ruslan Álvarez-Diduk**: visualization (equal); writing—original draft (equal); and writing—review and editing (supporting). **Arben Merkoçi**: funding acquisition (equal); supervision (equal); writing—original draft (supporting); and writing—review and editing (supporting). **Majlinda Vasjari**: funding acquisition (equal) and writing—review and editing (supporting). **Lueda Kulla**: writing—original draft (supporting) and writing—review and editing (supporting). **Michal Otyepka**: conceptualization (lead); funding acquisition (equal); project administration (lead); supervision (lead); visualization (supporting); writing—original draft (lead); and writing—review and editing (lead).

Keywords: biosensors · covalent immobilizations · electrochemistries · graphenes · inkjet printings

[1] K. J. Land, D. I. Boeras, X.-S. Chen, A. R. Ramsay, R. W. Peeling, *Nat. Microbiol.* **2019**, *4*, 46.
[2] L. C. Clark, C. Lyons, *Ann. N. Y. Acad. Sci.* **1962**, *102*, 29.
[3] R. Renneberg, D. Pfeiffer, F. Lisdat, G. Wilson, U. Wollenberger, F. Ligler, A. P. F. Turner, in *Biosensing 21st Century*, (Eds: R. Renneberg, F. Lisdat), Springer Berlin Heidelberg, Berlin, Heidelberg **2008**, pp. 1–18.
[4] A. Amine, F. Arduini, D. Moscone, G. Palleschi, *Biosens. Bioelectron.* **2016**, *76*, 180.
[5] J. He, E. Spanolios, C. E. Froehlich, C. L. Wouters, C. L. Haynes, *ACS Sens.* **2023**, *8*, 1391.
[6] C. I. L. Justino, A. C. Duarte, T. A. P. Rocha-Santos, *TrAC - Trends Anal. Chem.* **2016**, *85*, 36.
[7] B. Li, H. Tan, D. Jenkins, V. Srinivasa Raghavan, B. G. Rosa, F. Güder, G. Pan, E. Yeatman, D. J. Sharp, *Carbon* **2020**, *168*, 144.
[8] J. Peña-Bahamonde, H. N. Nguyen, S. K. Fanourakis, D. F. Rodrigues, *J. Nanobiotechnol.* **2018**, *16*, 75.
[9] F. Risse, E. T. Gedig, J. S. Gutmann, *Anal. Bioanal. Chem.* **2018**, *410*, 4109.
[10] K. Edward Sekhosana, S. A. Majeed, U. Feleni, *Coord. Chem. Rev.* **2023**, *491*, 215232.
[11] Y. Gao, I. Kyratzis, *Bioconjugate Chem.* **2008**, *19*, 1945.
[12] H. M. Pineda-Castañeda, Z. J. Rivera-Monroy, M. Maldonado, *ACS Omega* **2023**, *8*, 3650.
[13] N. Z. Fantoni, A. H. El-Sagheer, T. Brown, *Chem. Rev.* **2021**, *121*, 7122.
[14] M. A. Morales, J. M. Halpern, *Bioconjugate Chem.* **2018**, *29*, 3231.
[15] L. C. Lopes, A. Santos, P. R. Bueno, *Sens. Actuators Rep.* **2022**, *4*, 100087.
[16] C. Nieto, M. A. Vega, E. M. Martín del Valle, *Nanomaterials* **2020**, *10*, 1674.
[17] N. Elgrishi, K. J. Rountree, B. D. McCarthy, E. S. Rountree, T. T. Eisenhart, J. L. Dempsey, *J. Chem. Educ.* **2018**, *95*, 197.
[18] K. Scott, in *Microb. Electrochem. Fuel Cells*, (Eds: K. Scott, E. H. Yu), Woodhead Publishing, Boston, **2016**, pp. 29–66.
[19] B. Limoges, J.-M. Savéant, *J. Electroanal. Chem.* **2003**, *549*, 61.
[20] A. A. Sehat, A. A. Khodadadi, F. Shemirani, Y. Mortazavi, *Int. J. Electrochem. Sci.* **2015**, *10*, 272.
[21] H. Liu, C. Tao, Z. Hu, S. Zhang, J. Wang, Y. Zhan, *RSC Adv.* **2014**, *4*, 43624.
[22] C. S. Movassaghi, K. A. Perrotta, H. Yang, R. Iyer, X. Cheng, M. Dagher, M. A. Fillol, A. M. Andrews, *Anal. Bioanal. Chem.* **2021**, *413*, 6747.
[23] S. Rantataro, I. Parkkinen, M. Airavaara, T. Laurila, *Biosens. Bioelectron.* **2023**, *241*, 115579.
[24] I. S. da Silva, B. Capovilla, K. H. G. Freitas, L. Angnes, *Anal. Methods* **2013**, *5*, 3546.
[25] A. Chen, B. Shah, *Anal. Methods* **2013**, *5*, 2158.
[26] S. W. Abeykoon, R. J. White, *ACS Meas. Sci. Au* **2023**, *3*, 1.

[27] M. Yuan, S. Qian, H. Cao, J. Yu, T. Ye, X. Wu, L. Chen, F. Xu, *Food Chem.* **2022**, *382*, 132173.
[28] E. P. Randviir, C. E. Banks, *Anal. Methods* **2022**, *14*, 4602.
[29] H. S. Magar, R. Y. A. Hassan, A. Mulchandani, *Sensors* **2021**, *21*, 6578.
[30] X. Liu, X. Qu, J. Dong, S. Ai, R. Han, *Biosens. Bioelectron.* **2011**, *26*, 3679.
[31] A. K. Shukla, J. S. Boruah, S. Park, B. Kim, *J. Phys. Chem. C* **2024**, *128*, 13458.
[32] A. C. Lazanas, M. I. Prodromidis, *ACS Meas. Sci. Au* **2023**, *3*, 162.
[33] F. Ciucci, *Curr. Opin. Electrochem.* **2019**, *13*, 132.
[34] A. Maradesa, B. Py, J. Huang, Y. Lu, P. Iurilli, A. Mrozinski, H. M. Law, Y. Wang, Z. Wang, J. Li, S. Xu, Q. Meyer, J. Liu, C. Brivio, A. Gavrilyuk, K. Kobayashi, A. Bertei, N. J. Williams, C. Zhao, M. Danzer, M. Zic, P. Wu, V. Yrjänä, S. Pereverzyev, Y. Chen, A. Weber, S. V. Kalinin, J. P. Schmidt, Y. Tsur, B. A. Boukamp, Q. Zhang, M. Gaberšček, R. O'Hayre, F. Ciucci, *Joule* **2024**, *8*, 1958.
[35] E. Vermisoglou, D. Panáček, K. Jayaramulu, M. Pykal, I. Frébort, M. Kolář, M. Hajdúch, R. Zbořil, M. Otyepka, *Biosens. Bioelectron.* **2020**, *166*, 112436.
[36] K. S. Novoselov, A. K. Geim, S. V. Morozov, D. Jiang, Y. Zhang, S. V. Dubonos, I. V. Grigorieva, A. A. Firsov, *Science* **2004**, *306*, 666.
[37] A. Gutiérrez-Cruz, A. R. Ruiz-Hernández, J. F. Vega-Clemente, D. G. Luna-Gazcón, J. Campos-Delgado, *J. Mater. Sci.* **2022**, *57*, 14543.
[38] Y. Zhang, L. Zhang, C. Zhou, *Acc. Chem. Res.* **2013**, *46*, 2329.
[39] Y. Zhu, S. Murali, W. Cai, X. Li, J. W. Suk, J. R. Potts, R. S. Ruoff, *Adv. Mater.* **2010**, *22*, 3906.
[40] N. Kumar, R. Salehiyan, V. Chauke, O. Joseph Botlhoko, K. Setshedi, M. Scriba, M. Masukume, S. Sinha Ray, *FlatChem* **2021**, *27*, 100224.
[41] P. T. Araujo, M. Terrones, M. S. Dresselhaus, *Mater. Today* **2012**, *15*, 98.
[42] M. D. Bhatt, H. Kim, G. Kim, *RSC Adv.* **2022**, *12*, 21520.
[43] D. Chen, H. Feng, J. Li, *Chem. Rev.* **2012**, *112*, 6027.
[44] A. Ambrosi, C. K. Chua, N. M. Latiff, A. H. Loo, C. H. A. Wong, A. Y. S. Eng, A. Bonanni, M. Pumera, *Chem. Soc. Rev.* **2016**, *45*, 2458.
[45] M. Pumera, *Electrochem. Commun.* **2013**, *36*, 14.
[46] A. Ambrosi, C. K. Chua, A. Bonanni, M. Pumera, *Chem. Rev.* **2014**, *114*, 7150.
[47] G. Seo, G. Lee, M. J. Kim, S.-H. Baek, M. Choi, K. B. Ku, C.-S. Lee, S. Jun, D. Park, H. G. Kim, S.-J. Kim, J.-O. Lee, B. T. Kim, E. C. Park, S. I. Kim, *ACS Nano* **2020**, *14*, 5135.
[48] V. Georgakilas, M. Otyepka, A. B. Bourlinos, V. Chandra, N. Kim, K. C. Kemp, P. Hobza, R. Zboril, K. S. Kim, *Chem. Rev.* **2012**, *112*, 6156.
[49] C. Wetzl, A. Silvestri, M. Garrido, H.-L. Hou, A. Criado, M. Prato, *Angew. Chem. Int. Ed.* **2023**, *62*, e202212857.
[50] R. A. Bueno, J. I. Martínez, R. F. Luccas, N. R. del Árbol, C. Munuera, I. Palacio, F. J. Palomares, K. Lauwaet, S. Thakur, J. M. Baranowski, W. Strupinski, M. F. López, F. Mompean, M. García-Hernández, J. A. Martín-Gago, *Nat. Commun.* **2017**, *8*, 15306.
[51] J. Greenwood, T. H. Phan, Y. Fujita, Z. Li, O. Ivasenko, W. Vanderlinden, H. Van Gorp, W. Frederickx, G. Lu, K. Tahara, Y. Tobe, H. Uji-i, S. F. L. Mertens, S. De Feyter, *ACS Nano* **2015**, *9*, 5520.
[52] C. Wetzl, S. Brosel-Oliu, M. Carini, D. Di Silvio, X. Illa, R. Villa, A. Guimera, E. Prats-Alfonso, M. Prato, A. Criado, *Nanoscale* **2023**, *15*, 16650.
[53] D. C. Elias, R. R. Nair, T. M. G. Mohiuddin, S. V. Morozov, P. Blake, M. P. Halsall, A. C. Ferrari, D. W. Boukhvalov, M. I. Katsnelson, A. K. Geim, K. S. Novoselov, *Science* **2009**, *323*, 610.
[54] W. S. Hummers, R. E. Offeman, *J. Am. Chem. Soc.* **1958**, *80*, 1339.
[55] J. Chen, B. Yao, C. Li, G. Shi, *Carbon* **2013**, *64*, 225.
[56] D. C. Marcano, D. V. Kosynkin, J. M. Berlin, A. Sinitskii, Z. Sun, A. Slesarev, L. B. Alemany, W. Lu, J. M. Tour, *ACS Nano* **2010**, *4*, 4806.
[57] X. Chen, Z. Qu, Z. Liu, G. Ren, *ACS Omega* **2022**, *7*, 23503.
[58] C. Giacomelli, R. Álvarez-Diduk, A. Testolin, A. Merkoçi, *2D Mater.* **2020**, *7*, 024006.
[59] A. Scroccarello, R. Álvarez-Diduk, F. Della Pelle, C. De Carvalho Castro, E. Silva, A. Idili, C. Parolo, D. Compagnone, A. Merkoçi, *ACS Sens.* **2023**, *8*, 598.
[60] E. Calucho, R. Álvarez-Diduk, A. Piper, M. Rossetti, T. K. Nevanen, A. Merkoçi, *Biosens. Bioelectron.* **2024**, *258*, 116315.
[61] D. Echeverri, E. Calucho, J. Marrugo-Ramírez, R. Álvarez-Diduk, J. Orozco, A. Merkoçi, *Biosens. Bioelectron.* **2024**, *252*, 116142.
[62] B. L. Garrote, A. Santos, P. R. Bueno, *Nat. Protoc.* **2020**, *15*, 3879.
[63] P. R. Bueno, J. J. Davis, *Chem. Soc. Rev.* **2020**, *49*, 7505.
[64] Q. Wang, Z. Zhou, Y. Zhai, L. Zhang, W. Hong, Z. Zhang, S. Dong, *Talanta* **2015**, *141*, 247.
[65] H. S. Dinani, M. Pourmadadi, F. Yazdian, H. Rashedi, S. A. S. Ebrahimi, J. S. Shayeh, M. Ghorbani, *Eng. Life Sci.* **2022**, *22*, 519.
[66] H. Yu, W. Guo, X. Lu, H. Xu, Q. Yang, J. Tan, W. Zhang, *Food Control* **2021**, *127*, 108117.
[67] S. K. Krishnan, E. Singh, P. Singh, M. Meyyappan, H. S. Nalwa, *RSC Adv.* **2019**, *9*, 8778.
[68] G. Gopal, N. Roy, A. Mukherjee, *Biosensors* **2023**, *13*, 488.
[69] D. D. Chronopoulos, A. Bakandritsos, M. Pykal, R. Zbořil, M. Otyepka, *Appl. Mater. Today* **2017**, *9*, 60.
[70] R. R. Nair, W. Ren, R. Jalil, I. Riaz, V. G. Kravets, L. Britnell, P. Blake, F. Schedin, A. S. Mayorov, S. Yuan, M. I. Katsnelson, H. Cheng, W. Strupinski, L. G. Bulusheva, A. V. Okotrub, I. V. Grigorieva, A. N. Grigorenko, K. S. Novoselov, A. K. Geim, *Small* **2010**, *6*, 2877.
[71] D. K. Samarakoon, Z. Chen, C. Nicolas, X. Wang, *Small* **2011**, *7*, 965.
[72] F. Karlický, M. Otyepka, *Ann. Phys.* **2014**, *526*, 408.
[73] V. Hrubý, L. Zdražil, J. Dzíbelová, V. Šedajová, A. Bakandritsos, P. Lazar, M. Otyepka, *Appl. Surf. Sci.* **2022**, *587*, 152839.
[74] D. Matochová, M. Medveď, A. Bakandritsos, T. Steklý, R. Zbořil, M. Otyepka, *J. Phys. Chem. Lett.* **2018**, *9*, 3580.
[75] M. Medveď, G. Zoppellaro, J. Ugolotti, D. Matochová, P. Lazar, T. Pospíšil, A. Bakandritsos, J. Tuček, R. Zbořil, M. Otyepka, *Nanoscale* **2018**, *10*, 4696.
[76] Q. Yang, E. P. Nguyen, D. Panáček, V. Šedajová, V. Hrubý, G. Rosati, C. D. C. Castro Silva, A. Bakandritsos, M. Otyepka, A. Merkoçi, *Green Chem.* **2023**, *25*, 1647.
[77] D. Panáček, L. Zdražil, M. Langer, V. Šedajová, Z. Baďura, G. Zoppellaro, Q. Yang, E. P. Nguyen, R. Álvarez-Diduk, V. Hrubý, J. Kolařík, N. Chalmpes, A. B. Bourlinos, R. Zbořil, A. Merkoçi, A. Bakandritsos, M. Otyepka, *Small* **2022**, *31*, 2201003.
[78] J. M. R. Flauzino, E. P. Nguyen, Q. Yang, G. Rosati, D. Panáček, A. G. Brito-Madurro, J. M. Madurro, A. Bakandritsos, M. Otyepka, A. Merkoçi, *Biosens. Bioelectron.* **2022**, *195*, 113628.
[79] W. Feng, P. Long, Y. Feng, Y. Li, *Adv. Sci.* **2016**, *3*, 1500413.
[80] V. Hrubý, D. Zaoralová, M. Medveď, A. Bakandritsos, R. Zbořil, M. Otyepka, *Nanoscale* **2022**, *14*, 13490.
[81] D. D. Chronopoulos, M. Medveď, G. Potsi, O. Tomanec, M. Scheibe, M. Otyepka, *Chem. Commun.* **2020**, *56*, 1936.
[82] H. Barès, A. Bakandritsos, M. Medve, J. Ugolotti, P. Jakubec, O. Tomanec, S. Kalytchuk, R. Zbořil, M. Otyepka, *Carbon* **2019**, *145*, 251.
[83] A. Kouloumpis, D. D. Chronopoulos, G. Potsi, M. Pykal, J. Vlček, M. Scheibe, M. Otyepka, *Chem. – Eur. J.* **2020**, *26*, 6518.
[84] V. Šedajová, A. Bakandritsos, P. Błoński, M. Medveď, R. Langer, D. Zaoralová, J. Ugolotti, J. Dzíbelová, P. Jakubec, V. Kupka, M. Otyepka, *Energy Environ. Sci.* **2022**, *15*, 740.
[85] D. Zaoralová, V. Hrubý, V. Šedajová, R. Mach, V. Kupka, J. Ugolotti, A. Bakandritsos, M. Medved', M. Otyepka, *ACS Sustainable Chem. Eng.* **2020**, *8*, 4764.
[86] J. M. R. Flauzino, M.-A. Nalepa, D. D. Chronopoulos, V. Šedajová, D. Panáček, P. Jakubec, P. Kührová, M. Pykal, P. Banáš, A. Panáček, A. Bakandritsos, M. Otyepka, *Small* **2023**, *19*, 2370428.
[87] A. Bakandritsos, M. Pykal, P. Błoński, P. Jakubec, D. D. Chronopoulos, K. Poláková, V. Georgakilas, K. Čépe, O. Tomanec, V. Ranc, A. B. Bourlinos, R. Zbořil, M. Otyepka, *ACS Nano* **2017**, *11*, 2982.
[88] A. K. K. Padinjareveetil, M. Pykal, A. Bakandritsos, R. Zbořil, M. Otyepka, M. Pumera, *Adv. Sci.* **2024**, *11*, 2307583.
[89] V. Hrubý, V. Šedajová, P. Jakubec, A. Bakandritsos, R. Zbořil, M. Otyepka, *Power Electron. Devices Compon.* **2024**, *7*, 100058.
[90] V. Šedajová, P. Jakubec, A. Bakandritsos, V. Ranc, M. Otyepka, *Nanomaterials* **2020**, *10*, 1731.
[91] J. Jumper, R. Evans, A. Pritzel, T. Green, M. Figurnov, O. Ronneberger, K. Tunyasuvunakool, R. Bates, A. Žídek, A. Potapenko, A. Bridgland, C. Meyer, S. A. A. Kohl, A. J. Ballard, A. Cowie, B. Romera-Paredes, S. Nikolov, R. Jain, J. Adler, T. Back, S. Petersen, D. Reiman, E. Clancy, M. Zielinski, M. Steinegger, M. Pacholska, T. Berghammer, S. Bodenstein, D. Silver, O. Vinyals, A. W. Senior, K. Kavukcuoglu, P. Kohli, D. Hassabis, *Nature* **2021**, *596*, 583.
[92] B. Schneider, B. A. Sweeney, A. Bateman, J. Cerny, T. Zok, M. Szachniuk, *Nucl. Acids Res.* **2023**, *51*, 9522.
[93] J. Šponer, G. Bussi, M. Krepl, P. Banáš, S. Bottaro, R. A. Cunha, A. Gil-Ley, G. Pinamonti, S. Poblete, P. Jurečka, N. G. Walter, M. Otyepka, *Chem. Rev.* **2018**, *118*, 4177.
[94] M. Mondal, L. Yang, Z. Cai, P. Patra, Y. Q. Gao, *Chem. Sci.* **2021**, *12*, 5390.
[95] M. Paloncýová, M. Pykal, P. Kührová, P. Banáš, J. Šponer, M. Otyepka, *Small* **2022**, *18*, 2204408.
[96] B. Mohr, T. Van Heesch, A. Pérez De Alba Ortíz, J. Vreede, *WIREs Comput. Mol. Sci.* **2024**, *14*, e1712.
[97] Q. Li, J. P. Froning, M. Pykal, S. Zhang, Z. Wang, M. Vondrák, P. Banáš, K. Čépe, P. Jurečka, J. Šponer, R. Zbořil, M. Dong, M. Otyepka, *2D Mater.* **2018**, *5*, 031006.
[98] M. Malhotra, M. Puglia, A. Kalluri, D. Chowdhury, C. V. Kumar, *Sens. Actuators Rep.* **2022**, *4*, 100077.
[99] W. Peng, H. Li, Y. Liu, S. Song, *J. Mol. Liq.* **2017**, *230*, 496.

[100] Y. Zuo, J. Xu, X. Zhu, X. Duan, L. Lu, Y. Yu, *Microchim. Acta* **2019**, *186*, 171.
[101] M. Shabbir, Z. A. Raza, T. H. Shah, M. R. Tariq, *J. Nanostruct. Chem.* **2022**, *12*, 1033.
[102] S. R. Benjamin, E. J. Miranda Ribeiro Júnior, *Curr. Opin. Environ. Sci. Health* **2022**, *29*, 100381.
[103] F. Yin, W. Yue, Y. Li, S. Gao, C. Zhang, H. Kan, H. Niu, W. Wang, Y. Guo, *Carbon* **2021**, *180*, 274.
[104] D.-B. Moon, A. Bag, H. H. Chouhdry, S. J. Hong, N.-E. Lee, *ACS Sens.* **2024**, *9*, 6071.
[105] Y. Ravi Kumar, K. Deshmukh, T. Kovářík, S. K. Khadheer Pasha, *Coord. Chem. Rev.* **2022**, *461*, 214502.
[106] G. J. Thangamani, K. Deshmukh, T. Kovářík, N. A. Nambiraj, D. Ponnamma, K. K. Sadasivuni, H. P. S. A. Khalil, S. K. K. Pasha, *Chemosphere* **2021**, *280*, 130641.
[107] H. R. Ansari, A. Mirzaei, H. Shokrollahi, R. Kumar, J.-Y. Kim, H. W. Kim, M. Kumar, S. S. Kim, *J. Mater. Chem. C* **2023**, *11*, 6528.
[108] H. Chen, F. Zhuo, J. Zhou, Y. Liu, J. Zhang, S. Dong, X. Liu, A. Elmarakbi, H. Duan, Y. Fu, *Chem. Eng. J.* **2023**, *464*, 142576.
[109] Y. Qiao, X. Li, T. Hirtz, G. Deng, Y. Wei, M. Li, S. Ji, Q. Wu, J. Jian, F. Wu, Y. Shen, H. Tian, Y. Yang, T.-L. Ren, *Nanoscale* **2019**, *11*, 18923.
[110] E. Singh, M. Meyyappan, H. S. Nalwa, *ACS Appl. Mater. Interfaces* **2017**, *9*, 34544.
[111] H. Zhang, R. He, Y. Niu, F. Han, J. Li, X. Zhang, F. Xu, *Biosens. Bioelectron.* **2022**, *197*, 113777.
[112] A. Silvestri, C. Wetzl, N. Alegret, L. Cardo, H.-L. Hou, A. Criado, M. Prato, *Adv. Drug Delivery Rev.* **2022**, *186*, 114315.
[113] S. Cinti, F. Arduini, *Biosens. Bioelectron.* **2017**, *89*, 107.
[114] F. Arduini, L. Micheli, D. Moscone, G. Palleschi, S. Piermarini, F. Ricci, G. Volpe, *TrAC Trends Anal. Chem.* **2016**, *79*, 114.
[115] M. Sher, A. Faheem, W. Asghar, S. Cinti, *TrAC Trends Anal. Chem.* **2021**, *143*, 116374.
[116] Y. Chu, C. Qian, P. Chahal, C. Cao, *Adv. Sci.* **2019**, *6*, 1801653.
[117] A. Silvestri, A. Criado, F. Poletti, F. Wang, P. Fanjul-Bolado, M. B. González-García, C. García-Astrain, L. M. Liz-Marzán, X. Feng, C. Zanardi, M. Prato, *Adv. Funct. Mater.* **2022**, *32*, 2105028.
[118] K. E. Lee, in *Sustainable Text. Ind.*, (Ed: S. S. Muthu), Springer, Singapore, **2017**, pp. 17–55.
[119] G. Hu, J. Kang, L. W. T. Ng, X. Zhu, R. C. T. Howe, C. G. Jones, M. C. Hersam, T. Hasan, *Chem. Soc. Rev.* **2018**, *47*, 3265.
[120] P. Yang, H. J. Fan, *Adv. Mater. Technol.* **2020**, *5*, 2000217.
[121] D. McManus, S. Vranic, F. Withers, V. Sanchez-Romaguera, M. Macucci, H. Yang, R. Sorrentino, K. Parvez, S.-K. Son, G. Iannaccone, K. Kostarelos, G. Fiori, C. Casiraghi, *Nat. Nanotechnol.* **2017**, *12*, 343.
[122] K. Zub, S. Hoeppener, U. S. Schubert, *Adv. Mater.* **2022**, *34*, 2105015.
[123] J. Li, J. Liu, W. Huo, J. Yu, X. Liu, M. J. Haslinger, M. Muehlberger, P. Kulha, X. Huang, *Mater. Today Nano* **2022**, *18*, 100201.
[124] X. Yang, Y. Lin, T. Wu, Z. Yan, Z. Chen, H.-C. Kuo, R. Zhang, *Opto-Electron. Adv.* **2022**, *5*, 210123.
[125] D. Lohse, *Annu. Rev. Fluid Mech.* **2022**, *54*, 349.
[126] M. Franco, A. Motealleh, C. M. Costa, L. Hilliou, N. Perinka, C. Ribeiro, J. C. Viana, P. Costa, S. Lanceros-Mendez, *Adv. Eng. Mater.* **2022**, *24*, 2101258.
[127] M.-A. Nalepa, D. Panáček, I. Dědek, P. Jakubec, V. Kupka, V. Hrubý, M. Petr, M. Otyepka, *Biosens. Bioelectron.* **2024**, *256*, 116277.
[128] T. Juntunen, H. Jussila, M. Ruoho, S. Liu, G. Hu, T. Albrow-Owen, L. W. T. Ng, R. C. T. Howe, T. Hasan, Z. Sun, I. Tittonen, *Adv. Funct. Mater.* **2018**, *28*, 1800480.
[129] S. Majee, M. Song, S.-L. Zhang, Z.-B. Zhang, *Carbon* **2016**, *102*, 51.
[130] T. Kant, K. Shrivas, K. Dewangan, A. Kumar, N. K. Jaiswal, M. K. Deb, S. Pervez, *Mater. Today Chem.* **2022**, *24*, 100769.
[131] M. Jafarpour, F. Nüesch, J. Heier, S. Abdolhosseinzadeh, *Small Sci.* **2022**, *2*, 2200040.
[132] A. Silvestri, S. Vázquez-Díaz, G. Misia, F. Poletti, R. López-Domene, V. Pavlov, C. Zanardi, A. L. Cortajarena, M. Prato, *Small* **2023**, *19*, 2300163.

Manuscript received: November 30, 2024
Revised manuscript received: March 17, 2025
Version of record online: